

Copolymerization of Styrene and Methyl Methacrylate in Ternary Oil-in-Water Microemulsions: Monomer Reactivity Ratios and Microstructures by ^1H NMR and ^{13}C NMR

L. M. Gan, K. C. Lee, C. H. Chew, S. C. Ng,* and L. H. Gan†

Department of Chemistry, National University of Singapore,
Kent Ridge, Singapore 0511, Republic of Singapore

Received May 20, 1994*

ABSTRACT: The monomer reactivity ratios of styrene (r_S) and methyl methacrylate (r_M) copolymerization in ternary oil-in-water microemulsions were determined from the ^1H NMR spectra. The obtained values of $r_S = 0.74 \pm 0.09$ and $r_M = 0.38 \pm 0.04$ are different from those determined by homogeneous polymerizations. The results are discussed in terms of the partitioning of monomers in the microemulsions and the copolymerization loci. Information about the microstructures of copolymers was derived from the analysis of the methoxyl region of the ^1H NMR spectra and the α -methyl region as well as the aromatic C1 region of the ^{13}C NMR spectra. The experimental results on the copolymer microstructures are in good agreement with the calculated values using the newly determined r_S and r_M . The glass transition temperatures (T_g) of the copolymers were found to decrease linearly with increasing mole fraction of styrene in the copolymers.

Introduction

Microemulsions,¹ in contrast to emulsions, are thermodynamically stable, transparent dispersions of oil or water stabilized by larger amounts of surfactant (>5 wt %) and often with an alcohol cosurfactant. Microemulsion polymerization is a process that can produce polymer particles of high molecular weights (10^5 – 10^7) but small sizes (20–80 nm in diameter). The simplest microemulsion system for polymerization contains only monomer, water, and surfactant. The polymerization kinetics for the ternary-component microemulsions are easier to analyze, because of the absence of effects of an alcohol cosurfactant on the partitioning² of monomer and chain-transfer reactions.³ Ferrick et al.⁴ were the first to report on the polymerization of styrene in a ternary-component microemulsion in 1989. Since then, several works on polymerizations of styrene,^{5–8} methyl methacrylate (MMA),^{9,10} and tetrahydrofurfuryl methacrylate¹¹ in different ternary-component microemulsions have been reported.

Candau et al.^{12,13} showed that the reactivity ratios of copolymerizations of both water-soluble monomer acrylamide (M_1) and sodium acrylate (M_2) in inverse microemulsions were close to unity. This is significantly different from the literature values ($r_1 \sim 0.95$, $r_2 \sim 0.30$) obtained from copolymers prepared in a solution or an inverse emulsion. However, monomer reactivity ratios for the copolymerization of styrene and MMA in microemulsions containing only monomer, water, and surfactant are still not available in the literature. The objective of this paper is to report information about these monomer reactivity ratios as well as the microstructures of styrene–MMA (SM) copolymers determined by ^1H NMR and ^{13}C NMR.

Experimental Section

Materials. Tetradecyltrimethylammonium bromide (TTAB) purchased from TCI (Japan) was recrystallized from an ethanol–acetone mixture. Potassium persulfate (KPS) from Fluka was

recrystallized from doubly distilled water. Styrene (Fluka) and MMA (Fluka) were purified by vacuum distilled at 3 mmHg at 20 °C.

Copolymerization. Microemulsion copolymerizations were carried out at 60 °C using 0.15 mM KPS. The compositions of microemulsions were 7 wt % mixed monomers (varying the feed molar ratio of monomers styrene and MMA), 9 wt % TTAB, and 84 wt % water. The copolymer samples at low conversion (below 7%) were precipitated by a large quantity of methanol. They were purified by repeated washing with methanol and then vacuum dried for 24 h.

Copolymer Characterization. The compositions of the copolymers were determined by ^1H NMR and ^{13}C NMR. ^1H NMR spectra were recorded with a Bruker AMX 500 spectrometer operating at 500 MHz and 298 K, using CDCl_3 as solvent with a sample concentration of ca. 2% (w/v) and TMS as an internal reference. Spectra were run with a 5 s pulse recycle time at a 45° pulse angle. The 125 MHz ^{13}C NMR spectra were recorded with the same spectrometer using the WALTZ-16 decoupling procedure at 298 K. The sample concentration was ca. 5% (w/v) in CDCl_3 solution. The ^{13}C NMR spectra were also run at a 45° pulse angle with a 5 s pulse recycle time to ensure that all the carbon-13 nuclei were completely relaxed. Spectra were obtained by accumulating 5000–8000 scans.

The glass transition temperatures (T_g) of the copolymers were measured using a Perkin-Elmer DSC-4 differential scanning calorimeter with a heating rate of 20 °C/min. The initial onset of the slope of the DSC curve was taken as T_g .

Results and Discussion

Monomer Reactivity Ratios of Styrene (r_S) and MMA (r_M). Figure 1 is a typical ^1H NMR spectrum of a SM copolymer, while Figure 2 shows only the expanded methoxyl regions for a series of SM copolymers obtained at low conversions. The protons of the phenyl group appeared around chemical shift $\delta = 7$ ppm. The styrene composition in a copolymer was calculated from the peak area of the protons due to the phenyl group (A_p) and the total area of all protons (A_t); i.e., the mole fraction of styrene in a copolymer is $F_S = 8A_p/5A_t$.

The feed and the calculated compositions of styrene and MMA in the copolymers are summarized in Table 1. The monomer reactivity ratios for r_S and r_M were evaluated using the Fineman–Ross¹⁴ and the Kelen–Tudos¹⁵ meth-

* To whom correspondence should be addressed at the Department of Physics, National University of Singapore.

† Division of Chemistry, NIE, Nanyang Technological University.

• Abstract published in *Advance ACS Abstracts*, September 1, 1994.

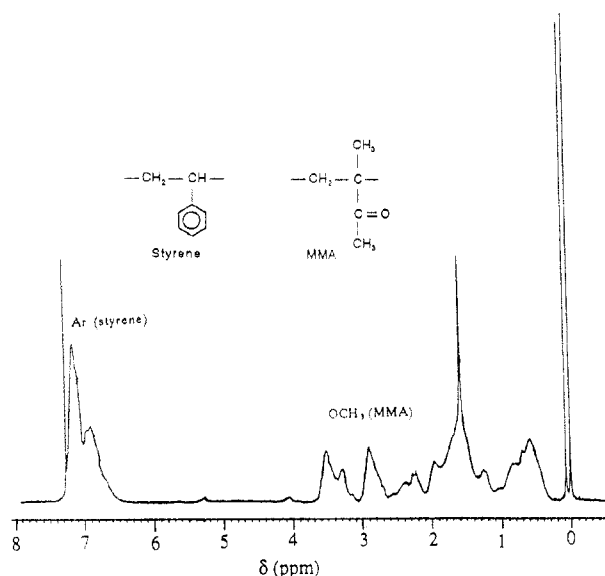


Figure 1. ^1H NMR spectrum of SM60 copolymer in CDCl_3 at 298 K.

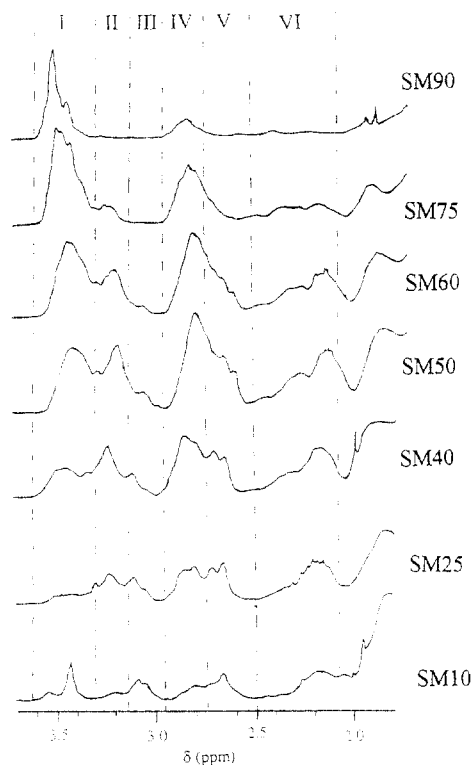


Figure 2. Expanded ^1H NMR spectra of the methoxyl region of the SM copolymers.

ods. Except for the higher feed ratios of styrene (SM10 and SM25), good linear plots were obtained for other compositions by both methods. It was found that $r_S = 0.73$ and $r_M = 0.38$ by the Fineman–Ross method and $r_S = 0.74$ and $r_M = 0.38$ by the Kelen–Tudos method. According to the method of error analysis of Kelen and Tudos,¹⁶ $\Delta r_S = \pm 0.09$ and $\Delta r_M = \pm 0.04$ were obtained. These monomer reactivity ratios of styrene and MMA in microemulsion polymerization are different from those obtained by homogeneous (bulk or solution) copolymerization as shown in Table 2. It should be noted that r_S (0.74) from microemulsion copolymerization is larger than those from the conventional methods (homogeneous copolymerization), but the reverse applies for r_M (0.38 vs 0.45). These results are of great interest because they may provide some information about the mechanism of copolymerization of styrene and MMA in microemulsions.

Table 1. Compositions of Styrene and MMA in the Feeds and Copolymers^a

system	f_S	f_M	F_S	F_M	conv (wt %)
SM10	0.90	0.10	0.82	0.18	3.21
SM25	0.74	0.26	0.66	0.34	6.35
SM40	0.59	0.41	0.62	0.38	1.38
SM50	0.49	0.51	0.55	0.45	2.58
SM60	0.39	0.61	0.49	0.51	1.98
SM75	0.24	0.76	0.36	0.64	1.89
SM90	0.10	0.90	0.19	0.81	2.82

^a Microemulsion compositions: 9 wt % TTAB, 84 wt % water, 7 wt % of mixed styrene and MMA with various molar ratios and 0.15 mM KPS. Polymerized temperature = 60 °C. f_S and f_M : mole fractions of styrene and MMA in the feeds, respectively. F_S and F_M : mole fractions of styrene and MMA in the copolymers, respectively.

Table 2. Monomer Reactivity Ratios of Styrene and MMA from Different Methods of Copolymerization

polymerization method	reactivity ratios		ref
	r_S	r_M	
bulk	0.50 ± 0.03	0.45 ± 0.3	17
bulk	0.48 ± 0.03	0.42 ± 0.09	18
bulk	0.52	0.46	19
bulk	0.47	0.45	20–21
solution	0.50 ± 0.02	0.44 ± 0.02	22
microemulsion	0.74 ± 0.09	0.38 ± 0.04	this work

Table 3. Distributions of Styrene and MMA in Microemulsions before Polymerization^a

system	f_S/f_M	f'_S/f'_M	f'_M	f'_M/f'_S	S_M (wt %)
SM10	9.00	11.97	0.08	0.75	0.17
SM25	2.85	3.79	0.20	0.75	0.45
SM40	1.44	1.91	0.31	0.75	0.71
SM50	0.96	1.28	0.38	0.75	0.89
SM60	0.64	0.85	0.46	0.75	1.06
SM75	0.32	0.43	0.57	0.75	1.32
SM90	0.11	0.14	0.68	0.76	1.56

^a f_S/f_M : styrene/MMA molar ratio in the feed. f'_S/f'_M : calculated styrene/MMA molar ratio in polymerization loci. f'_M/f'_S : molar ratio of MMA in polymerization loci to MMA in the feed. S_M : weight percent of MMA solubilized in the aqueous phase based on the total weight of each microemulsion system.

The monomer reactivity ratios of r_S and r_M from microemulsion copolymerizations can be related to those from bulk or solution copolymerizations as follows:²²

$$r_S = r'_S/k_{SM}; \quad r_M = r'_M/k_{SM}$$

$$f'_S/f'_M = k_{SM}(f_S/f_M)$$

where r'_S (0.50) and r'_M (0.45) are those from bulk copolymerization,¹⁸ f_S/f_M is the styrene/MMA molar ratio in the feed, and k_{SM} and f'_S/f'_M are the distribution coefficient and the styrene/MMA molar ratio in the polymerization loci, respectively. The values of k_{SM} were calculated from the first two equations, and the average value of $k_{SM} = 1.33$ was used for the calculation of f'_S/f'_M .

Table 3 summarizes the information about the distributions of styrene and MMA in the microemulsion systems before polymerization. The calculated styrene/MMA molar ratios (f'_S/f'_M) in the polymerization loci are all higher than those in the feeds (f_S/f_M). This would imply that the copolymerization loci were in the microemulsion droplets, because the solubility of styrene (0.031 wt %) is much lower than that of MMA. The estimation of the MMA present in the polymerization loci (f'_M) is based on the assumption that all styrene added would be in the microemulsion droplets; i.e., $f'_S \approx f_S$. Although the mole fraction of added MMA (f_M) increased from 0.10 to 0.90

Table 4. Normalized Peak Areas (I–VI) of the Methoxyl Resonances of Styrene–MMA Copolymers^a

system	F_M	peak						
		I	II	III	IV	V	VI	
SM10	0.18	0.01	0.10	0.22	0.12	0.38	0.18	calcd
		0.04	0.11	0.21	0.15	0.29	0.20	obsd
SM25	0.34	0.07	0.18	0.11	0.23	0.25	0.15	calcd
		0.10	0.18	0.10	0.28	0.16	0.17	obsd
SM40	0.38	0.18	0.19	0.05	0.30	0.16	0.12	calcd
		0.18	0.18	0.06	0.34	0.08	0.16	obsd
SM50	0.45	0.27	0.18	0.03	0.31	0.11	0.10	calcd
		0.27	0.16	0.02	0.35	0.05	0.14	obsd
SM60	0.51	0.37	0.15	0.01	0.31	0.07	0.08	calcd
		0.37	0.12	0.01	0.36	0.03	0.11	obsd
SM75	0.64	0.56	0.09	0.00	0.27	0.03	0.04	calcd
		0.51	0.08	0.00	0.33	0.01	0.07	obsd
SM90	0.81	0.80	0.02	0.00	0.16	0.00	0.01	calcd
		0.73	0.02	0.00	0.22	0.00	0.03	obsd

^a F_M : mole fraction of MMA in copolymers.

for samples SM10 to SM90, the molar ratios of MMA present in the polymerization loci to the feed MMA (f_M'/f_M) remained almost constant at 0.75 for all systems. This means that only 75% of added MMA was present in the polymerization loci. The remaining 25% was solubilized in the aqueous phase of the microemulsion system. Based on this information, the calculated amount of MMA solubilized in the aqueous phase increased from 0.17 to 1.56 wt % (based on the total weight percent of the microemulsion) for samples SM10 to SM90 as shown in Table 3. It is surprising to note that the highest solubility of MMA (1.56 wt %) calculated for sample SM90 is identical to the maximum solubility of MMA in water reported in the literature.²³ This means that the calculated value of 0.75 for f_M'/f_M is valid. From these calculations, it can be concluded that the monomer reactivity ratios of microemulsions were determined by the styrene/MMA molar ratio in the microenvironment of the polymerization loci (microemulsion droplets) rather than the feed molar ratio.

Microstructures of Copolymers. ¹H NMR Method.

Assignments of a ¹H NMR spectrum of a statistical SM copolymer (Figure 1) have been discussed by Ito,^{24–26} Bovey,²⁷ Uebel,¹⁷ Kale,^{20,21} and German et al.²⁸ Among these, the assignments by German et al.²⁸ produce the most satisfactory results. Their assignments are based on a MMA-centered pentad sequence. The peak areas are designated I–VI, which are due to combined compositional (or sequence) and configurational (or tacticity) effects as shown in Figure 2. The MMA-centered pentad sequence can be evaluated from the Alfrey–Mayo equations²⁹ using the monomer reactivity ratio ($r_M = 0.38$) obtained from this microemulsion polymerization.

The theoretical relative peak areas calculated according to German's assignments²⁸ (peaks I–VI in Figure 2) are presented in Table 4, together with the experimental values for comparison. The experimental results are in good agreement with the calculated peak areas. This confirms that $r_M = 0.38$ obtained from the microemulsion copolymerization is reliable.

¹³C NMR Method. Figure 3 shows the NMR spectrum of SM60 copolymer. The expanded spectra of the α -methyl region of the MMA unit ($\delta = 22$ –16) and the aromatic C1 region for the styrene unit ($\delta = 147$ –143) are shown in Figure 4. These are four distinct peaks in the α -methyl region, i.e., A ($\delta = 22.0$ –21.0), B ($\delta = 21.0$ –19.3), C ($\delta = 19.3$ –17.2), and D ($\delta = 17.2$ –16.0), and three peaks in the C1 region, namely, X ($\delta = 147.0$ –146.2), Y ($\delta = 146.2$ –144.8), and Z ($\delta = 144.8$ –143.0). The assignments for these

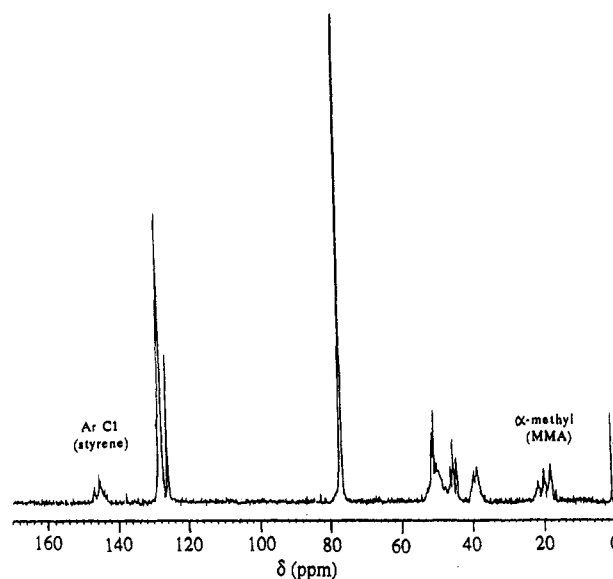


Figure 3. ¹³C NMR spectrum of SM60 copolymer in CDCl₃ at 298 K.

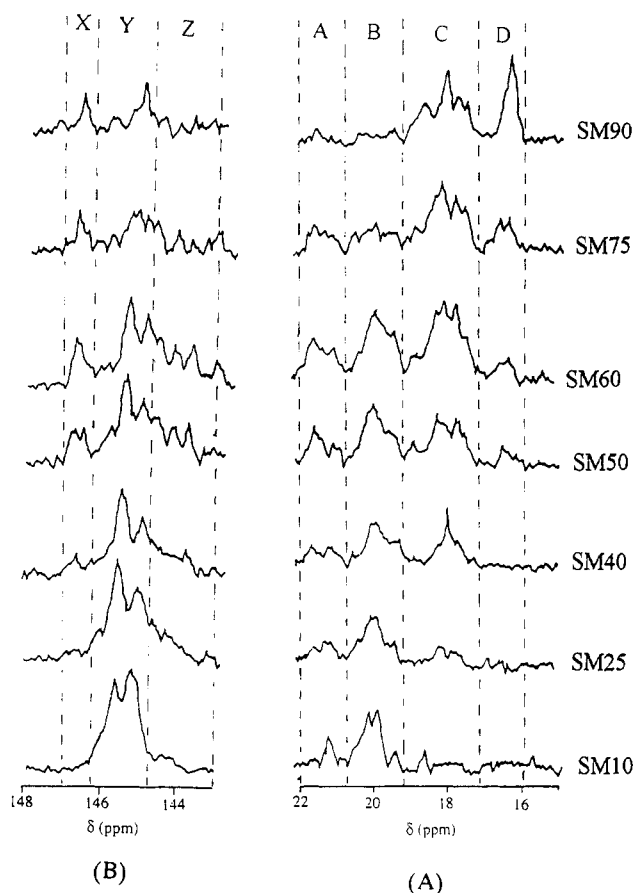


Figure 4. Expanded ¹³C NMR spectra of the SM copolymers: (A) α -methyl peak; (B) aromatic C1 peak.

peaks were based on those reported by Katritzky et al.³⁰ and German et al.³¹ It is found that the assignments by German et al. give better results than those by Katritzky et al. as compared to the experimental values. Hence, the subsequent treatments of the results are based only on the assignments by German et al., as give in Table 5. It should be noted that the configuration of $(1 - \sigma_{SM})^2 F_{SMS}$ was split between peak areas B and C. Thus, peaks B and C can be considered as one. Based on these assignments and the monomer reactivity ratios of $r_S = 0.74$ and $r_M = 0.38$, the calculated and the experimental values of the peak areas are in good agreement, as shown in Table 6.

Table 5. Assignments³¹ of ¹³C NMR Spectra for Statistical SM Copolymers

α -CH ₃ peak chem shift (ppm) config	A 22.0–21.0 $\sigma_{MM}^2 F_{MMM}$ $\sigma_{MM}\sigma_{SM} F_{MMS}$ $\sigma_{SM}^2 F_{SMS}$	B 21.0–19.3 $\sigma_{MM}(1 - \sigma_{SM}) F_{MMS}$ $2\sigma_{SM}(1 - \sigma_{SM}) F_{SMS}$ $(1 - \sigma_{SM})^2 F_{SMS}^a$	C 19.3–17.2 $2\sigma_{MM}(1 - \sigma_{MM}) F_{MMM}$ $(1 - \sigma_{MM})\sigma_{SM} F_{MMS}$ $(1 - \sigma_{MM})(1 - \sigma_{SM}) F_{MMS}$ $(1 - \sigma_{SM})^2 F_{SMS}^a$	D 17.2–16.0 $(1 - \sigma_{MM})^2 F_{MMM}$
C1 peak chem shift (ppm) config	X 147–146.2 $(1 - \sigma_{SM})^2 F_{MSM}$	Y 146.2–144.8 $\sigma_{SS}^2 F_{SSS}$ $2\sigma_{SS}(1 - \sigma_{SS}) F_{SSS}$ $(1 - \sigma_{SS})^2 F_{SSS}$ $\sigma_{SS}(1 - \sigma_{SM}) F_{SSM}$ $2\sigma_{SM}(1 - \sigma_{SM}) F_{MSM}$ $(1 - \sigma_{SM})(1 - \sigma_{SS}) F_{SSM}$	Z 144.8–143.0 $(1 - \sigma_{SS})\sigma_{SM} F_{SSM}$ $\sigma_{SS}\sigma_{SM} F_{SSM}$ $\sigma_{SM}^2 F_{MSM}$	

^a The peak shows resonance splitting and appears in both B and C peak areas. σ_{ij} ($i, j = S$ or M) is the coisotacticity parameter, and $\sigma_{MM} = 0.23$, $\sigma_{SM} = 0.44$, and $\sigma_{SS} = 0.29$. F_{ijk} ($i, j, k = S$ or M) is the mole fraction of triads in copolymers.

Table 6. Normalized Peak Areas of the α -Methyl and Aromatic C1 Resonances of SM Copolymers

	α -methyl peak			aromatic C1 peak			
	A	B + C	D	X	Y	Z	
SM10	0.19	0.81	0.00	0.01	0.89	0.11	calcd
	0.19	0.81	0.00	0.02	0.89	0.09	obsd
SM25	0.17	0.82	0.00	0.03	0.76	0.21	calcd
	0.18	0.82	0.00	0.05	0.73	0.22	obsd
SM40	0.16	0.82	0.03	0.07	0.66	0.27	calcd
	0.18	0.77	0.05	0.07	0.67	0.26	obsd
SM50	0.14	0.81	0.05	0.11	0.61	0.28	calcd
	0.16	0.78	0.06	0.12	0.62	0.27	obsd
SM60	0.13	0.79	0.08	0.14	0.58	0.28	calcd
	0.15	0.78	0.06	0.14	0.57	0.28	obsd
SM75	0.11	0.72	0.18	0.20	0.53	0.26	calcd
	0.11	0.75	0.15	0.20	0.56	0.23	obsd
SM90	0.08	0.56	0.36	0.27	0.50	0.23	calcd
	0.08	0.54	0.38	0.26	0.52	0.22	obsd

Table 7. Calculated and Observed Fractions of Styrene- and MMA-Centered Triads in SM Copolymers

system	styrene-centered triads			MMA-centered triads			
	F_{SSS}	F_{SSM}	F_{MSM}	F_{MMM}	F_{MMS}	F_{SMS}	
SM10	0.75	0.23	0.02	0.00	0.08	0.92	calcd
($F_M = 0.18$)	0.76	0.19	0.05	0.00	0.09	0.91	obsd
SM25	0.46	0.43	0.11	0.01	0.21	0.78	calcd
($F_M = 0.34$)	0.41	0.43	0.16	0.00	0.21	0.79	obsd
SM40	0.27	0.50	0.23	0.04	0.33	0.62	calcd
($F_M = 0.38$)	0.28	0.49	0.23	0.08	0.40	0.51	obsd
SM50	0.17	0.49	0.34	0.08	0.41	0.51	calcd
($F_M = 0.45$)	0.19	0.44	0.37	0.10	0.50	0.41	obsd
SM60	0.10	0.44	0.46	0.14	0.47	0.39	calcd
($F_M = 0.51$)	0.10	0.44	0.46	0.11	0.54	0.35	obsd
SM75	0.04	0.31	0.65	0.30	0.50	0.21	calcd
($F_M = 0.64$)	0.11	0.25	0.64	0.25	0.55	0.20	obsd
SM90	0.01	0.14	0.86	0.61	0.34	0.05	calcd
($F_M = 0.81$)	0.03	0.13	0.84	0.64	0.28	0.08	obsd

The number fractions of various triads (F_{SSS} , F_{SSM} , F_{MSM} , F_{MMM} , F_{MMS} , and F_{SMS}) can be calculated from the Alfrey-Mayo equations²⁹ using monomer reactivity ratios of $r_S = 0.74$ and $r_M = 0.38$. The experimental triads were evaluated based on the data in Tables 5 and 6, which are in reasonably good agreement with the calculated values, as shown in Table 7. This can be better seen from Figure 5, which shows the variation of triad fractions as a function of mole fractions of styrene in the copolymer (F_S).

The number-average sequence lengths (N_S and N_M) can be evaluated from the fractions of diads and triads.²⁹ Moreover, the block character (K) of the copolymer can also be calculated from the following equation:³²

$$K = \frac{F_{SM}}{2F_SF_M}$$

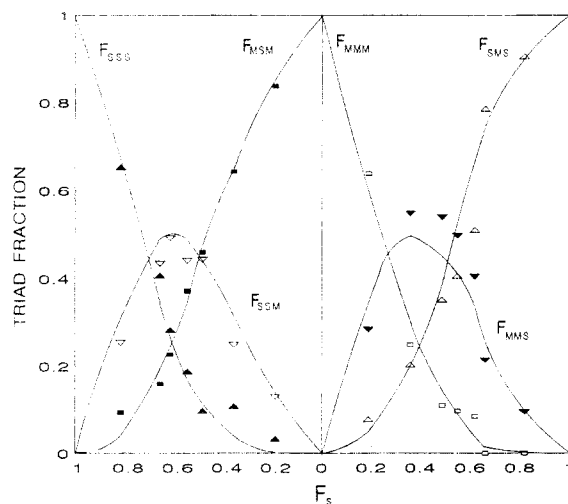


Figure 5. Normalized statistical monomer sequence distribution of triad fractions of styrene in the SM copolymers. Experimental data: (\blacktriangle) F_{SSS} ; (∇) F_{SSM} ; (\blacksquare) F_{MSM} ; (\square) F_{MMM} ; (\blacktriangledown) F_{SMS} ; (\triangle) F_{MMS} . The lines are calculated results based on $r_S = 0.74$ and $r_M = 0.38$.

Table 8. Copolymerization Parameters of Styrene-MMA Copolymers^a

system	F_{SS}	F_{SM}	F_{MM}	N_S	N_M	K	
SM10	0.71	0.29	0.01	5.96	1.05	0.96	calcd
	0.70	0.29	0.01	5.77	1.05	0.98	obsd
SM25	0.45	0.51	0.04	2.76	1.16	1.14	calcd
	0.41	0.55	0.04	2.49	1.13	1.23	obsd
SM40	0.31	0.60	0.08	2.01	1.27	1.27	calcd
	0.32	0.56	0.11	2.16	1.38	1.19	obsd
SM50	0.23	0.64	0.13	1.71	1.40	1.30	calcd
	0.22	0.62	0.16	1.72	1.50	1.25	obsd
SM60	0.16	0.65	0.19	1.47	1.60	1.30	calcd
	0.16	0.65	0.19	1.48	1.60	1.30	obsd
SM75	0.07	0.58	0.35	1.24	2.20	1.26	calcd
	0.08	0.58	0.33	1.29	2.15	1.26	obsd
SM90	0.01	0.35	0.63	1.08	4.57	1.15	calcd
	0.02	0.35	0.63	1.11	4.63	1.14	obsd

^a Calculated values are based on $r_S = 0.74$ and $r_M = 0.38$.

where F_S and F_M are the mole fractions of styrene and MMA in the copolymers, while F_{SM} is the diad fraction. When $0 \leq K \leq 1$, it reflects more block character of copolymers, whereas if $1 < K < 2$, it means more alternating tendency.

The values of the diad mole fractions (F_{SS} , F_{SM} , and F_{MM}), N_S , N_M , and K are listed in Table 8. For sample SM10, the values of F_{SS} and N_S are the highest among the SM copolymers due to its highest f_S (0.90). Thus, copolymer SM10 exhibited a more block character (K close to unity) with about 5 styrene units in a block unit. On

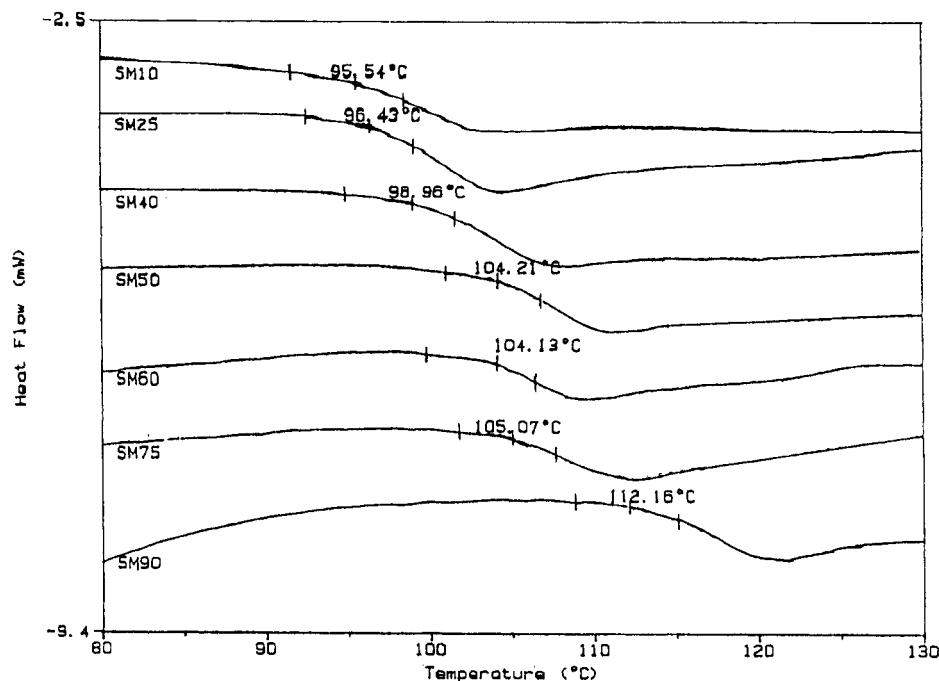


Figure 6. DSC measurements of the SM copolymers.

Table 9. Glass Transition Temperatures (T_g) for SM Copolymers

system	T_g (K)	
	exptl	calcd from Barton eqn
SM10	368.69	363.18
SM25	369.58	369.77
SM40	372.11	371.74
SM50	377.36	373.49
SM60	377.28	374.76
SM75	378.22	377.81
SM90	385.31	383.37

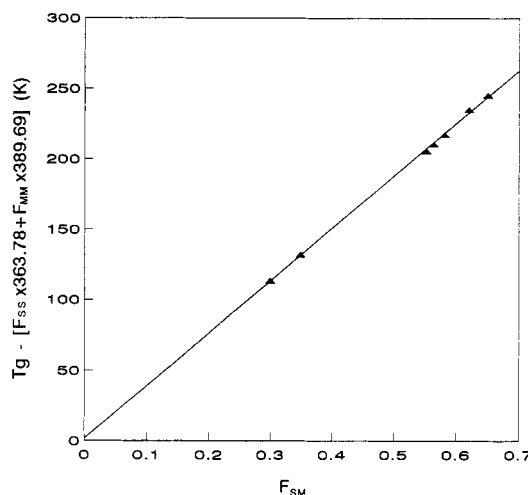
the other hand, sample SM90 produced the highest values of F_{MM} and N_M , implying that a block unit of 4–5 MMA monomer units was formed at $f_M = 0.90$. The highest value of F_{SM} was obtained for SM60, and the number-average sequence lengths of styrene (N_S) and MMA (N_M) were about the same. In addition, its highest values of K (1.30) indicated the alternating tendency for MMA and styrene in copolymer SM60.

Glass Transition Temperature (T_g). The variations of the glass transition temperature for the SM copolymers are recorded by the DSC measurements as shown in Figure 6 and they are summarized in Table 9. The T_g decreased linearly with increasing fraction of styrene in the copolymers. Barton³³ suggested that T_g is affected by the sequential distribution of monomeric units of a linear copolymer, and it is given by the following equation:

$$T_g = F_{SS}T_{g,SS} + F_{MM}T_{g,MM} + F_{SM}T_{g,SM}$$

where $T_{g,MM}$ and $T_{g,SS}$ are the T_g of PMMA and polystyrene (PS), respectively. $T_{g,MM}$ (116.54 °C) and $T_{g,SS}$ (90.63 °C) were obtained from the intercepts of the plot of T_g vs F_S .

The plot of $[T_g - (F_{SS}T_{g,SS} + F_{MM}T_{g,MM})]$ vs F_{SM} (Figure 7) shows a linear relationship passing through the origin, and a value of 372.92 K for $T_{g,SM}$ was obtained from the slope of the plot. This value of $T_{g,SM}$ was subsequently used for calculating the T_g 's of SM copolymers with various mole fractions of diads according to Barton's equation. The experimental values of T_g for the SM copolymers are in good agreement with the calculated values, as shown in Table 9.

Figure 7. Plot of $[T_g - (F_{SS}T_{g,SS} + F_{MM}T_{g,MM})]$ vs F_{SM} for the SM copolymers. The line is a linear least-squares fit.

Conclusions

The monomer reactivity ratios of styrene and MMA obtained from microemulsion copolymerization ($r_S = 0.74 \pm 0.09$ and $r_M = 0.38 \pm 0.04$) are different from those obtained from homogeneous copolymerizations. The difference arises from the partitioning of MMA in microemulsion droplets and in the aqueous phases of the microemulsion systems. The copolymerization is believed to be carried out inside the microemulsion droplets.

The information about the microstructures of the SM copolymers analyzed by the ^1H NMR and ^{13}C NMR spectra is in good agreement with the calculated values based on the monomer reactivity ratios $r_S = 0.74$ and $r_M = 0.38$. This confirms the reliability of the monomer reactivity ratios of styrene and MMA obtained from the copolymerization in ternary oil-in-water microemulsions.

References and Notes

- (1) Candau, F. *Encyclopedia of Polymer Science and Engineering*; Mark, H. F., Bikales, N. M., Overberger, C. G., Menges, G., Eds.; John Wiley: New York, 1987; Vol. 9, p 718.
- (2) Guo, J. S.; Sudol, E. D.; Vanderhoff, J. W.; El-Aasser, M. S. *J. Polym. Sci., Part A: Polym. Chem.* 1992, 30, 691.

- (3) Gan, L. M.; Chew, C. H.; Lye, I.; Ma, L.; Li, G. *Polymer* **1993**, *34*, 3860.
- (4) Ferrick, M. R.; Murtagh, J.; Thomas, J. K. *Macromolecules* **1989**, *22*, 1515.
- (5) Pérez-Luna, V. H.; Puig, J. E.; Castano, V. M.; Rodriguez, B. E.; Murthy, A. K.; Kaler, E. W. *Langmuir* **1990**, *6*, 1040.
- (6) Antonietti, M.; Bremser, W.; Müschenborn, D.; Rosenauer, C.; Schupp, B.; Schmidt, M. *Macromolecules* **1991**, *24*, 6636.
- (7) Antonietti, M.; Lohmann, S.; Van Niel, C. *Macromolecules* **1992**, *25*, 1139.
- (8) Gan, L. M.; Chew, C. H.; Lee, K. C.; Ng, S. C. *Polymer* **1994**, *35*, 2659.
- (9) Gan, L. M.; Chew, C. H.; Lee, K. C.; Ng, S. C. *Polymer* **1993**, *34*, 3064.
- (10) Gan, L. M.; Chew, C. H.; Ng, S. C.; Loh, S. E. *Langmuir* **1993**, *9*, 2799.
- (11) Full, A. P.; Puig, J. E.; Gron, L. U.; Kaler, E. W.; Minter, J. R.; Mourey, T. H.; Texter, J. *Macromolecules* **1992**, *25*, 5157.
- (12) Candau, F.; Zekhnini, Z.; Heatley, F. *Macromolecules* **1986**, *19*, 1895.
- (13) Candau, F.; Zekhnini, Z.; Heatley, F.; Franta, E. *Colloid Polym. Sci.* **1986**, *264*, 676.
- (14) Fineman, M.; Ross, S. D. *J. Polym. Sci.* **1950**, *5*, 269.
- (15) Kelen, T.; Tudos, F. *J. Macromol. Sci., Chem.* **1975**, *A9*, 1.
- (16) Kelen, T.; Tudos, F.; Turcsanyi, B. *Polym. Bull.* **1980**, *2*, 71.
- (17) Uebel, J. J.; Dinan, F. J. *J. Polym. Sci., Polym. Chem. Ed.* **1983**, *21*, 2427.
- (18) Maxwell, I. A.; Aerdt, A. M.; German, A. L. *Macromolecules* **1993**, *26*, 1956.
- (19) Fukuda, T.; Ma, Y.-D.; Inagaki, H. *Macromolecules* **1985**, *18*, 17.
- (20) O'Driscoll, K. F.; Kale, L. T.; Rubio, L. H. G.; Reilly, P. M. *J. Polym. Sci., Polym. Chem. Ed.* **1984**, *22*, 2777.
- (21) Kale, L. T.; O'Driscoll, K. F.; Dinan, F. J.; Uebel, J. J. *J. Polym. Sci., Part A: Polym. Chem. Ed.* **1986**, *24*, 3145.
- (22) Wall, F. T.; Florin, R. E.; Delbecq, C. J. *J. Am. Chem. Soc.* **1950**, *72*, 4769.
- (23) Riddick, A. J.; Bunger, W. B.; Sakano, J. K. *Organic Solvents*, 4th ed.; Wiley-Interscience: New York, 1986; Vol. II, p 423.
- (24) Ito, K.; Yamashita, Y. *J. Polym. Sci.* **1965**, *B3*, 625.
- (25) Ito, K.; Iwase, S.; Umehara, K.; Yamashita, Y. *J. Macromol. Sci., Chem.* **1967**, *A1*, 891.
- (26) Yamashita, Y.; Ito, K. *Appl. Polym. Symp.* **1969**, *8*, 245.
- (27) Bovey, F. A. *J. Polym. Sci.* **1962**, *62*, 197.
- (28) Aerdt, A. M.; de Haan, J. W.; German, A. L.; Van der Welden, G. P. M. *Macromolecules* **1991**, *24*, 1473.
- (29) Koenig, J. L. *Chemical Microstructure of Polymer Chains*; Wiley: New York, 1980; Chapter 3.
- (30) Katritzky, A. R.; Smith, A.; Weiss, D. E. *J. Chem. Soc., Perkin Trans. 2* **1974**, 1547.
- (31) Aerdt, A. M.; de Haan, J. W.; German, A. L. *Macromolecules* **1993**, *26*, 1965.
- (32) Brar, A. S.; Sunita, J. *Polym. Sci., Part A: Polym. Chem.* **1992**, *30*, 2549.
- (33) Barton, J. M. *J. Polym. Sci.* **1970**, *C30*, 573.